Int. J. Electrochem. Sci., 8 **(2013)** 7371 - 7380

International Journal of ELECTROCHEMICAL SCIENCE
www.electrochemsci.org

Crystallographic and Electrochemical Performances of $La_{0.7}Ce_{0.3}Ni_{3.65}Co_{0.1}Mn_{0.35}Al_{0.15}Cu_{0.75-x}V_x$ (x = 0.05-0.20) Alloys

Xianyun Peng[1], *Baozhong Liu*[1,*], *Yanping Fan*[1], *Liqiang Ji*[2], *Qian Li*[2], *Zhi Zhang*[1]

[1] School of Materials Science & Engineering, Henan Polytechnic University, Jiaozuo 454000, China
[2] Inner Mongolia Rare Earth Ovonic Metal Hydride Co. Ltd., Baotou 014030, China
[*]E-mail: bzliu@hpu.edu.cn

Received: 12 February 2013 / *Accepted:* 23 March 2013 / *Published:* 1 May 2013

Microstructures and electrochemical properties of $La_{0.7}Ce_{0.3}Ni_{3.65}Co_{0.1}Mn_{0.35}Al_{0.15}Cu_{0.75-x}V_x$ alloys are studied. X-ray diffraction results indicate that all alloys are identified with $LaNi_5$ phase with $CaCu_5$ type hexagonal structure. Calculated lattice parameter a, c and cell volume V increase, and a/c increases with increasing x value. Maximum discharge capacity of the alloy electrodes decreases from 322.9 mAh/g (x = 0.05) to 301.2 mAh/g (x = 0.20). High-rate dischargeability at the discharge current density of 1200 mA/g increases from 56.3% (x = 0.05) to 63.5% (x = 0.20). Cycling capacity retention rate at 100th cycles first increases from 69.9% (x = 0.05) to 72.3% (x = 0.10), and then decreases to 66.5% (x = 0.20), which should be ascribed to combined effect of advantageous and disadvantageous factors.

Keywords: Hydrogen storage alloy; Microstructures; Electrochemical property; Kinetics; Ni/MH batteries

1. INTRODUCTION

Nickel-metal hydride battery in which AB_5-type hydrogen storage alloy is employed as a negative electrode material has become a focus of interest as a candidate consumer-use battery by virtue of its several advantages: high reversible energy storage density, high resistance to overcharging and overdischarging, good charge-discharge kinetics, environmental compatibility and interchangeable, compared with nickel-cadmium battery [1-3]. However, wide application of Ni-MH battery is hindered due to the high cost of negative electrode materials. In order to decrease the raw cost, lots of Co-less or Co-free alloy was prepared by substituting with foreign metals, such as, Fe, Cu,

Si etc., whose raw cost was much cheaper than Co [4-6]. $La_{0.7}Ce_{0.3}Ni_{3.65}Co_{0.1}Mn_{0.35}Al_{0.15}Cu_{0.75}$ alloy was developed and commercially produced. However, the dischargeability is yet not satisfying. Thus, it is necessary to improve the electrochemical properties of the Co-less alloy.

Seo et al. [7, 8] reported that the discharge capacity and activation of $LaNi_{3.6}Al_{0.4}Co_{0.7}Mn_{0.3}V_y$ alloys can be improved by adding V if y is 0.02-0.1, and high-rate dischargeability was also enhanced due to the improvement in kinetic performance. The addition of V in $Mm(NiCoMnAlV)_5$ alloy also improved the discharge capacity and kinetic properties [9]. Obviously the addition of V element is effective to enhance the activation performance and dischargeability. Therefore, it can be expected that the electrochemical characteristics could be improved by substitution of V for Cu in Co-less alloys.

In this work, on the basis of the merits of V and the belief that the substitution of Cu by V may result in some noticeable modification of hydrogen storage properties, microstructures and electrochemical hydrogen storage properties of $La_{0.7}Ce_{0.3}Ni_{3.65}Co_{0.1}Mn_{0.35}Al_{0.15}Cu_{0.75-x}V_x$ (x = 0.05-0.20) alloys have been investigated systematically.

2. EXPERIMENTAL PROCEDURES

$La_{0.7}Ce_{0.3}Ni_{3.65}Co_{0.1}Mn_{0.35}Al_{0.15}Cu_{0.75-x}V_x$ (x = 0.05-0.20) alloys were synthesized by induction melting of the metal elements (La, Ce, Ni, Mn, Co, Al, V, Cu: 99.9% purity) in argon atmosphere and then were annealed at 1223 K for 10 h in argon atmosphere with the pressure of 0.08 MPa.

The phases of the alloy powders were determined by X-ray diffraction (XRD) using a Rigaku D/max 2500PC powder diffractometer with Cu Kα radiation. The microstructures of alloys were analyzed using Jade-5 software.

The alloy powders of measuring electrodes were obtained by grinding the inner part of alloy ingots in the argon atmosphere. All alloy electrodes for test were prepared by cold pressing the mixture of 0.15 g alloy powders of 200-400 meshes and 0.75 g nickel carbonyl powders into a pellet of 10 mm in diameter under 15 MPa. Electrochemical measurements were performed at 298 K in a standard tri-electrode system, consisting of a working electrode (metal hydride), a counter electrode ($Ni(OH)_2$/NiOOH), and a reference electrode (Hg/HgO) with 6mol/L KOH solution as electrolyte. Each electrode was charged for 7 h at 60 mA/g and discharged to -0.6 V versus Hg/HgO at 60 mA/g at 298 K. After every charging/discharging, the rest time was 10 min. In evaluating the high-rate dischargeability, discharge capacity of the alloy electrodes at different discharge current density was measured. The high-rate dischargeability HRD (%) defined as $C_n \times 100/(C_n + C_{60})$, was determined by the ratio of the discharge capacity C_n (n = 60, 300, 600, 900 and 1200) to the total discharge capacity defined as the sum of C_n and C_{60}, which was additional capacity measured subsequently at 60 mA/g after C_n was measured.

The linear polarization curve and potential-step measurement were obtained by Advanced Potentiostat/Galvanostat (PARSTAT 2273), respectively. Linear polarization curve was obtained by scanning the electrodes from -5 to 5 mV (vs. open circuit potential) at 50% depth of discharge (DOD).

For potential-step measurement, the electrodes in fully charged state were discharged with potential steps of +0.5 V for 3600 s.

3. RESULTS AND DISCUSSION

3.1. Microstructures

Fig. 1 shows the XRD patterns of $La_{0.7}Ce_{0.3}Ni_{3.65}Co_{0.1}Mn_{0.35}Al_{0.15}Cu_{0.75-x}V_x$ alloys. It shows that all alloys are identified with $LaNi_5$ phase with $CaCu_5$ type hexagonal structure. Calculated lattice parameters of the alloys are listed in Table 1. It can be seen that the lattice parameter *a*, *c* and cell volume *V* increase with increasing *x* value, and *c*/*a* value increases with increasing *x* value. This may be ascribed to the larger atomic radius of V (1.92 Å) than that of Cu (1.57 Å).

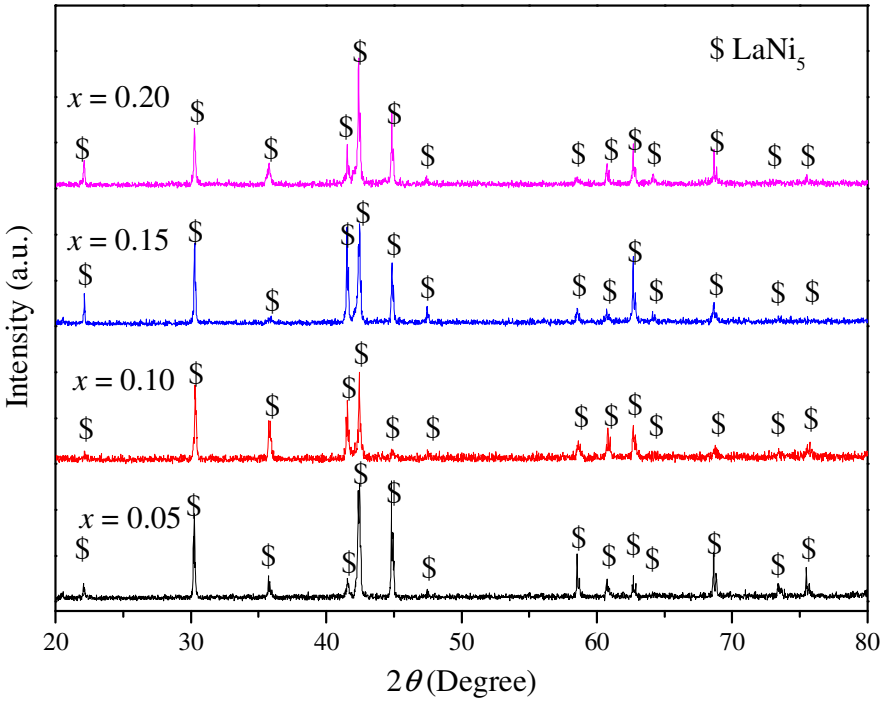

Figure 1. XRD of $La_{0.7}Ce_{0.3}Ni_{3.65}Co_{0.1}Mn_{0.35}Al_{0.15}Cu_{0.75-x}V_x$ alloys

Table 1. Lattice parameters of $La_{0.7}Ce_{0.3}Ni_{3.65}Co_{0.1}Mn_{0.35}Al_{0.15}Cu_{0.75-x}V_x$ alloys

x	*a*/Å	*c*/Å	*c*/*a*	*V*/Å^3
0.05	5.0151	4.0127	0.8001	87.40
0.10	5.0161	4.0178	0.8009	87.55
0.15	5.0176	4.0199	0.8011	87.64
0.20	5.0187	4.0213	0.8012	87.71

3.2 Activation capability and discharge capability

The number of cycles (N_a) needed to activate the electrodes and the maximum discharge capacity (C_{max}) of $La_{0.7}Ce_{0.3}Ni_{3.65}Co_{0.1}Mn_{0.35}Al_{0.15}Cu_{0.75-x}V_x$ alloy electrodes are given in Table 2. The N_a decreases from 5 (x = 0.05) to 2 (x = 0.20) with increasing x value, which indicates that the activation property is improved by increasing x value, which should be ascribed to the following factors. The V-dissolution makes the electrode surface of the alloys containing V change to microporous surface, which is very helpful to hydrogen penetration so that the fast initial activation occurs [7]. The increase in V content is beneficial to the activation property of the alloy electrodes. Moreover, Liu et al.[10] pointed out that the larger the unit cell volume resulted in the larger interstitial hole size for hydrogen atoms to occupy, which led to the smaller strain energy that hydrogen atoms to go in and out the crystal. The V of $LaNi_5$ phase increases with increasing x value, and then strain energy decreased, which is favorable for the activation performance of the alloys. The C_{max} of alloy electrodes decreases from 322.9 mAh/g (x = 0.05) to 301.2 mAh/g (x = 0.20). Generally speaking, maximum discharge capacity is related to the electrochemical kinetics and the stability of alloy hydride. Gao et al. [11] have reported the stability of alloy hydride was related to the stability of the hydride elements in alloy. The bond strength of V-H is stronger than that of Cu-H. The substitution of Cu by V will increase the stability of the alloy and then cause the hydrogen desorption more difficult, which decreased the discharge capacity. However, Brateng et al. [12] pointed out that the discharge capacity had a linear relationship with the cell volume. The larger the cell volume is, the discharge capacity is the higher. As mentioned above, the V of $LaNi_5$ phase increases with increasing x value, which is favorable to the discharge capacity. Thus, disadvantageous factor is prominent for the decrease in the C_{max} of alloy electrodes with increasing x value.

Table 1. Electrochemical property of $La_{0.7}Ce_{0.3}Ni_{3.65}Co_{0.1}Mn_{0.35}Al_{0.15}Cu_{0.75-x}V_x$ alloys

x	C_{max} (mAh/g)	N_a [b]	HRD_{1200} (%)	S_{100} (%)
0.05	322.9	5	56.3	69.9
0.10	316.0	3	58.5	72.3
0.15	311.2	3	60.6	68.1
0.20	301.2	2	63.5	66.5

[a] The high-rate dischargeability at the discharge current density of 1200 mA/g.

[b] The number of cycles needed to activate the electrode.

3.3 High-rate dischargeability and kinetics

Fig. 2 shows the relationship between the high-rate dischargeability (HRD) and the discharge current density of $La_{0.7}Ce_{0.3}Ni_{3.65}Co_{0.1}Mn_{0.35}Al_{0.15}Cu_{0.75-x}V_x$ alloy electrodes. The HRD of the alloy electrodes increases with increasing x from 0.05 to 0.20. The HRD at the discharge current density of

1200 mA/g (HRD_{1200}) is listed in Table 2. It can be seen that HRD_{1200} increases from 56.3% (x = 0.05) to 63.5% (x = 0.20).

It was well known that the HRD of the metal-hydride electrodes was dominated by the electrochemical kinetics of the charge-transfer reaction at the electrode/electrolyte interface and the hydrogen diffusion rate within the bulky alloy electrode, which were reflected in the value of the surface exchange current density (I_0), being a measure of the catalytic activity of an alloy, as well as in the hydrogen diffusion coefficient (D), which characterized the mass transport properties of an alloy electrode [13]. In order to examine the electrochemical kinetic properties, electrochemical impedance and potential-step experiment were performed on the investigated I-phase alloy electrodes.

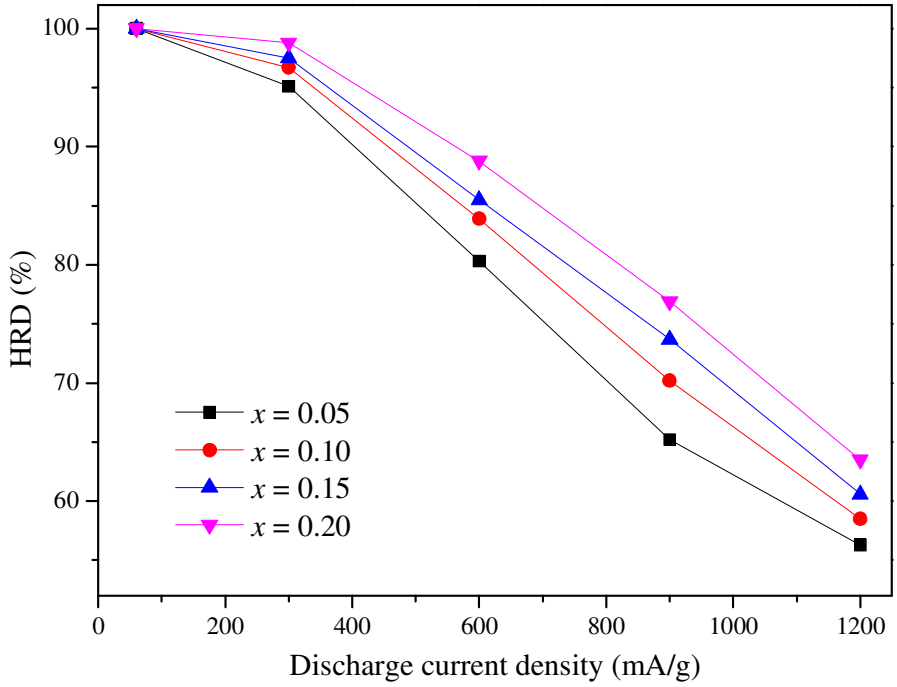

Figure 2. HRD of $La_{0.7}Ce_{0.3}Ni_{3.65}Co_{0.1}Mn_{0.35}Al_{0.15}Cu_{0.75-x}V_x$ alloy electrodes

Fig. 3 shows the linear polarization curves of $La_{0.73}Ce_{0.27}Ni_{3.25+x}Mn_{0.35}Al_{0.15}Cu_{0.75}Fe_{0.25}$ alloy electrodes at 50% DOD and 298 K. The polarization resistances (R_p) are calculated through estimating the slopes of linear polarization curves and listed in Table 3. The R_p values of the alloy electrodes decreases from 171.4 mΩ g (x = 0.05) to 153.2 mΩ g (x = 0.20). Besides, the I_0 value can be calculated according to the following formula [14].

$$I_0 = \frac{RT}{FR_p} \qquad (1)$$

where R, T, F, R_p are the gas constant, the absolute temperature, the Faraday constant and the polarization resistance, respectively.

Table 3. Electrochemical kinetic characteristics of $La_{0.7}Ce_{0.3}Ni_{3.65}Co_{0.1}Mn_{0.35}Al_{0.15}Cu_{0.75-x}V_x$ alloys

x	R_p (mΩ g)	I_0 (mA/g)	D ($\times 10^{-11}$ cm^2/s)
0.05	171.4	149.8	6.92
0.10	163.3	157.3	7.04
0.15	158.6	161.9	7.21
0.20	153.2	167.6	7.47

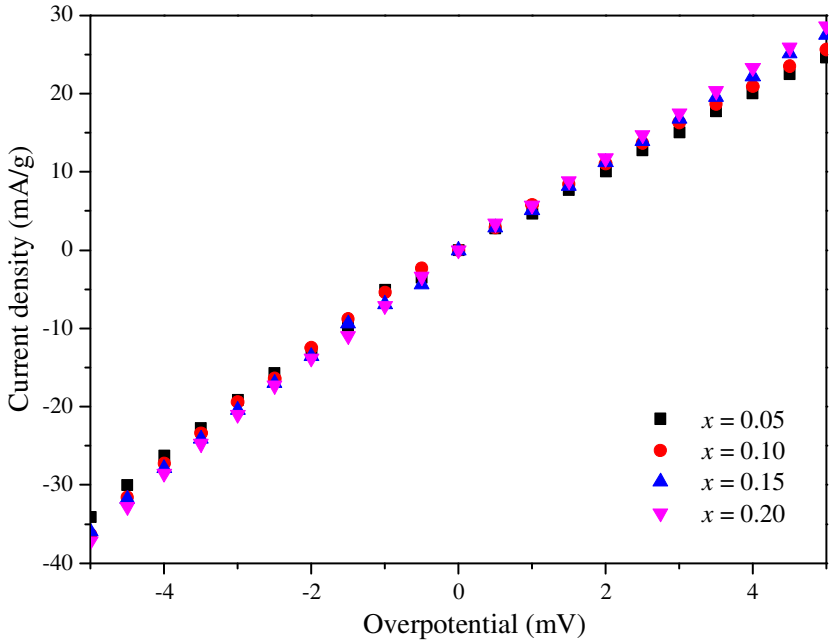

Figure 3. Linear polarization curves of $La_{0.7}Ce_{0.3}Ni_{3.65}Co_{0.1}Mn_{0.35}Al_{0.15}Cu_{0.75-x}V_x$ alloy electrodes at 50% DOD

The I_0 values are calculated by Eq. (1) and listed in Table 3. It is clear that the I_0 increases from 149.8 mA/g (x = 0.05) to 167.6 mA/g (x = 0.20). Li et al. [9] reported that the charge-transfer reaction can be speeded up by adding V in the AB_5-type alloy, which contributed to the charge-transfer reaction on the alloy surface. The increase in V content with increasing x value causes the improvement in charge-transfer reaction.

Fig. 4 shows the semi-logarithmic plots of the anodic current versus time response of the $La_{0.73}Ce_{0.27}Ni_{3.25+x}Mn_{0.35}Al_{0.15}Cu_{0.75}Fe_{0.25}$ alloy electrodes. Zheng et al. [15] reported that MH electrode reaction would be controlled by the rate of hydrogen diffusion in the bulk of alloys, when the rate of charge-transfer on the surface of alloy electrodes was so fast that the hydrogen concentration nearly equal to zero under a large anodic potential-step. Assuming that the grains of alloys are all spherical and the initial hydrogen concentration in the bulk of the alloy is even and the discharge

process of alloy electrode is an even system. When the discharge time is long enough, the hydrogen diffusion coefficient D can be calculated by the slope from the linear plot of log (i) versus t using the following formula:

$$\lg i = \lg(\frac{6FD}{da^2}(C_0 - C_s) - \frac{\pi^2}{2.303}\frac{D}{a^2}t \qquad (2)$$

where i is anodic current density (A/g), D the hydrogen diffusion coefficient (cm^2/s), d the density of the alloy (g/cm^3), a the radius of the alloy particle, C_0 the initial hydrogen concentration in the bulk of the alloy (mol/cm^3), C_s the surface hydrogen concentration of the alloy (mol/cm^3) and t is the discharge time (s). Assuming that the alloy has a similar particle distribution with an average particle radius of 13 □m according to previous study [16], D is calculated and summarized in Table 3. The D of $La_{0.7}Ce_{0.3}Ni_{3.65}Co_{0.1}Mn_{0.35}Al_{0.15}Cu_{0.75-x}V_x$ alloy electrodes increases from 6.92×10^{-11} cm^2/s (x = 0) to 7.47×10^{-10} cm^2/s (x = 0.75), which should be ascribed to the following factors. Firstly, Wang et al. [17] reported that the process of dissolved element V in the bulk into the electrolyte forms a 'path' and the diameter of formed 'path' is a little larger than hydrogen atom. This microporous surface caused by the V-dissolution is very helpful to hydrogen penetration [8]. The increase in V content will contribute to the improvement in hydrogen diffusion with increasing x value. Secondly, Yang et al. [18] pointed out that the increase in c/a ratio contributed to hydrogen going in and out of the crystal and imporved hydrogen diffusion. According to calculation result of lattice parameters, increasing x value causes the increase in the c/a ratio of $CaCu_5$-type phase and then makes hydrogen diffusion more easily.

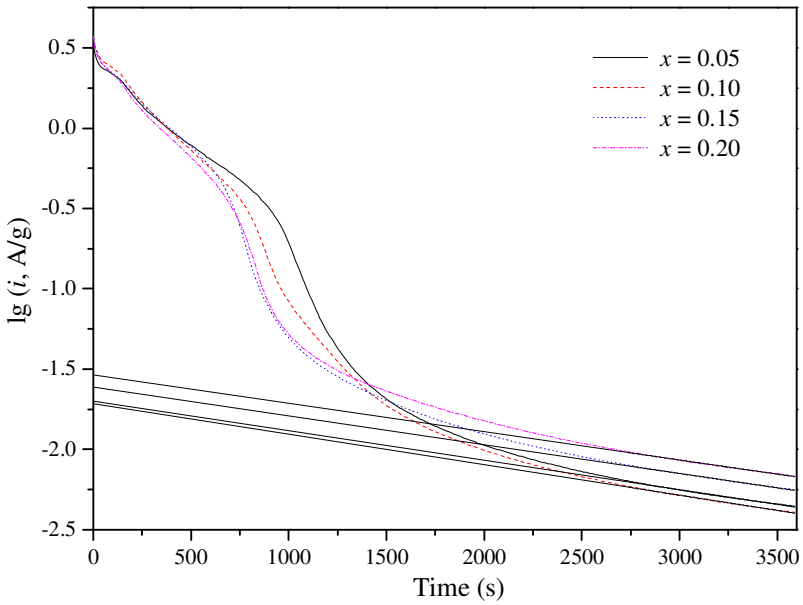

Figure 4. Semi-logarithmic plots of anodic current vs. time responses of $La_{0.7}Ce_{0.3}Ni_{3.65}Co_{0.1}Mn_{0.35}Al_{0.15}Cu_{0.75-x}V_x$ alloy electrodes

3.4 Cycling stability

The cycle stability is an extremely important factor for the service life of hydrogen storage alloys. The cycling capacity retention rate is expressed as $S_n(\%) = C_n/C_{max} \times 100$ (where C_n is the discharge capacity at the n^{th} cycle). The cycling capacity retention of the alloy electrode as a function of cycle number is shown in Fig. 5.

Clearly cycling stability first increases when x increases from 0.05 to 0.10, and then decreases until x increases to 0.20. The cycling capacity retention rate after 100 charge/discharge cycles (S_{100}) is listed in Table 2. It can be seen that S_{100} first increases from 69.9% ($x = 0.05$) to 72.3% ($x = 0.10$), and then decreases to 66.5% ($x = 0.20$). It is confirmed that the fundamental reasons for the capacity decay of the electrode alloy are pulverization of the alloy and the oxidation during charge-discharge cycle [19]. The increase of the *c/a* ratio facilitated hydrogen atoms from going in and out of the crystal and therefore decreased lattice stress during charge/discharge cycles [20]. The *c/a* ratio of the $LaNi_5$ phase increases with increasing x value, which contributes to anti-pulverization property and cycling stability of the alloy electrodes. Unfortunately, it is well-known that V dissolves easily in the KOH, which leads to the loss of discharge capacity. The increase in V content is unfavorable for the cycling stability of the alloy electrodes with increasing x value. Thus, it is reasonable to consider that the change in the cycling stability should be ascribed to the combined effect of advantageous and disadvantageous factors.

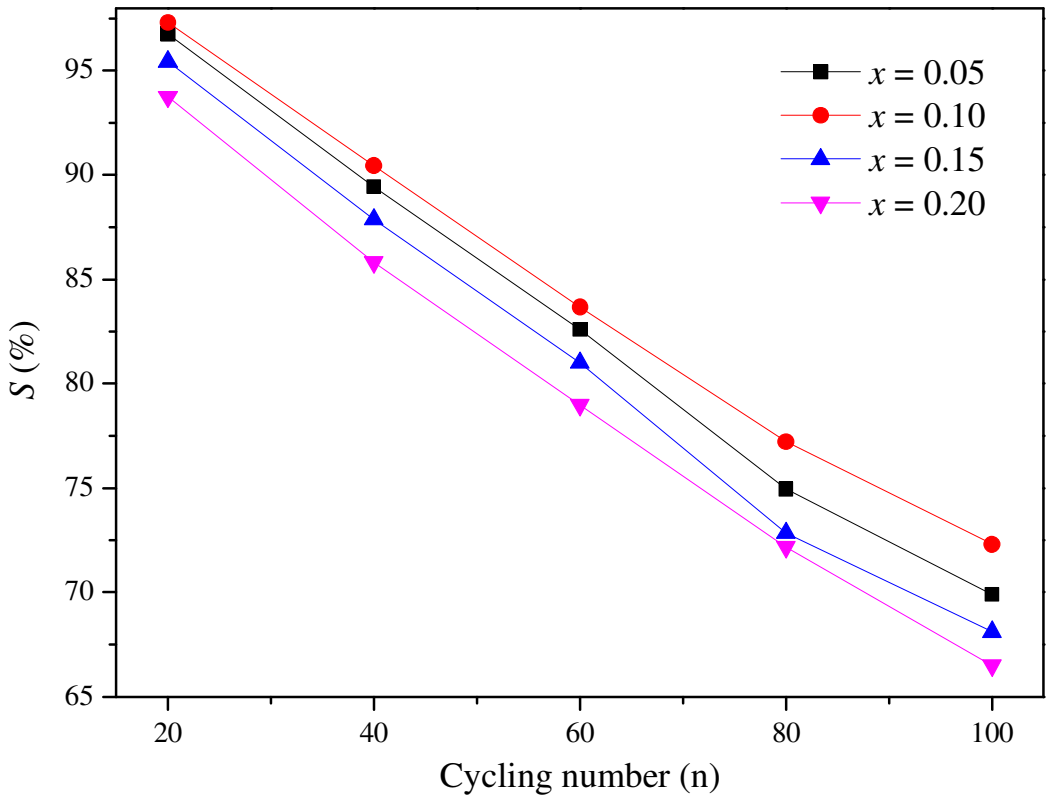

Figure 5. Cycling stability of $La_{0.7}Ce_{0.3}Ni_{3.65}Co_{0.1}Mn_{0.35}Al_{0.15}Cu_{0.75-x}V_x$ alloy electrodes

4. CONCLUSIONS

Microstructures and electrochemical properties of $La_{0.7}Ce_{0.3}Ni_{3.65}Co_{0.1}Mn_{0.35}Al_{0.15}Cu_{0.75-x}V_x$ alloys are investigated. XRD results indicate that all alloys are identified with $LaNi_5$ phase with $CaCu_5$ type hexagonal structure. Lattice parameter a, c and cell volume V decrease, and c/a increases with increasing x value. Maximum discharge capacity of the alloy electrodes decreases when x increases from 0 to 0.75. High-rate dischargeability of the alloy electrodes increases with increasing x from 0 to 0.75, which is attributed to the increase of I_0 and D. S_{100} first increases from 69.9% (x = 0.05) to 72.3% (x = 0.10), and then decreases to 66.5% (x = 0.20), which should be ascribed to the combined effect of advantageous and disadvantageous factors.

ACKNOWLEDGEMENTS
This research is financially supported by Program for Innovative Research Team (in Science and Technology) in the University of Henan Province (No. 2012IRTSTHN007), Baotou Science and Technology Project (2011J1003) and the Doctoral Foundation of Henan Polytechnic University (B2010-13).

References

1. T. Sakai, H. Yoshinaga, H. Migamura, N. Kurigama and H. Ishikawa, *J. Alloys Compd.*, 180 (1992) 37
2. Y. Fukumoto, M. Miyamoto, M. Matsuoka and C. Iwakura, *Electrochim. Acta*, 40 (1995) 845
3. S. Bliznakov, E. Lefterova, N. Dimitrov, K. Petrov and A. Popov, *J. Power Sources*, 176 (2008) 381
4. B. Liu, A.M. Liu, Y.P. Fan, M.J. Hu, B.Q. Zhang, *Trans. Nonferr. Metals Soc. of China*, 22 (2012) 1730.
5. S. Yang, S. Han, J.Z. Song and Y. Li, *J. Rare Earth*, 29 (2011) 692
6. S. Yang, S. Han, Y. Li and J.J. Liu, *Mater. Sci. Eng. B*, 178 (2013) 39
7. C.Y. Seo , S.J. Choi, J. Choi, C.N. Park, J.Y. Lee, *Int. J. Hydrogen Energy*, 28 (2003) 967.
8. C.Y. Seo , S.J. Choi, J. Choi, C.N. Park, J.Y. Lee, *J. Alloys Compd.*, 351 (2003) 255.
9. R. Li, J.M Wu, H. Su, S.X. Zhou, *J. Alloys Compd.*, 421 (2006) 258.
10. F.J. Liu, S. SUDA, *J. Alloys Compd.*, 232 (1996) 204.
11. X.P. Gao, Y. Wang, Z.W. Lu, F. Wu, D.Y. Song, P.W. Shen, *Chem. Mater.*, 16 (2004) 2515.
12. R. Brateng, S. Gulbrandsen-Dahl, L.O. Vaøen, J.K. Solberg, R. Tunold, *J. Alloys Compd.*, 396 (2005) 100.
13. B. Liu, M. Hu, L. Ji, Y. Fan, Y. Wang, Z. Zhang and A. Li, *J. Alloys Compd.*, 516 (2012) 53
14. P. Notten and P. Hokkeling, *J. Electrochem. Soc.*, 138 (1991) 1877
15. G. Zheng, B.N. Popov and R.E. White, *J. Electrochem. Soc.*, 142 (1995) 2695
16. B. Liu, Y. Zhang, G. Mi, Z. Zhang and L. Wang, *Int. J. Hydrogen Enegery*, 34 (2009) 6925
17. N. Wang, Y.J. Cai, *Rare Metal Mat. Eng.*, 40 (2011) 1519.
18. H. Yang, Y.G. Chen, M.D. Tao, C.L. Wu, *J. of Rare Earths*, 27 (2009) 853.

19. D. Chartouni, F. Meli, A. Zuttel, K. Gross and L. Schlapbach, *J. Alloys Compd.*, 241 (1996) 160
20. M. Takao, S. Satoshi, S. Naofumi, European Patent 1,075,032, A1(2001).